Kick-out diffusion of zinc in silicon at 1262 K

1989 J. Phys.: Condens. Matter 1 6347

(http://iopscience.iop.org/0953-8984/1/36/004)

J. Phys.: Condens. Matter 1 (1989) 6347–6361. Printed in the UK

Kick-out diffusion of zinc in silicon at 1262 K

M Perret†, N A Stolwijk† and L Cohausz‡§

† Institut für Metallforschung, Universität Münster, Wilhelm-Klemm-Strasse 10, D-4400 Münster, Federal Republic of Germany

‡ Institut für Technische Physik, Universität Kassel, Heinrich-Plett-Strasse 40, D-3500 Kassel, Federal Republic of Germany

Received 3 January 1989, in final form 15 May 1989

Abstract. Penetration profiles of Zn in Si were recorded with the aid of the spreading-resistance technique after in-diffusion from the vapour phase at 1262 K. The conversion of resistance data into concentrations of substitutional Zn is based on an acceptor level at $E_v + 0.24$ eV detected by Hall effect measurements on our Zn-diffused samples. The diffusion behaviour is found to be affected by surface conditions. In dislocation-free Si crystals with damaged surfaces the profile shape as well as the incorporation rate of Zn reveal a self-interstitial-limited diffusivity which depends on C^{-2}. Together with the much larger diffusion constant in highly dislocated samples this provides strong evidence that Zn in Si migrates by the kick-out mechanism.

1. Introduction

This study on the diffusion of Zn into Si was motivated by our previous experiments concerning the diffusion of the same transition metal in GaAs (Stolwijk *et al* 1988). Since Zn is used as the main acceptor dopant in GaAs and other III–V semiconductors, its transport properties in these materials are technologically extremely important. However, inspite of considerable efforts over the past three decades no real breakthrough with respect to the clarification of the diffusion mechanism of Zn in III–V compounds has been achieved. Therefore it appeared meaningful to us to examine for comparison the system Si:Zn where at least the experimental difficulties were expected to be much smaller.

Regarding GaAs:Zn there is general agreement that in the diffusion process exchanges of Zn atoms between interstitial and substitutional sites play a crucial role. We surveyed the much more limited literature on Zn in Si and in this case an interstitial–substitutional diffusion mechanism appears also to be possible. In fact this possibility has been suggested by several authors, without convincing evidence being given however.

As a simple criterion for interstitial–substitutional diffusion one may consider the magnitude of the diffusion coefficient. In well established examples of this migration mode, like Si:Au or Si:Pt, for example, the penetration rate lies between the slow diffusivities of the substitutional dopants and the fast mobilities of purely interstitial

§ Present address: Bio-Rad Laboratories GmbH, Dachauer Strasse 511, D-8000 München 50, Federal Republic of Germany.

0953-8984/89/366347+15$02.50

impurities. Remarkably, a similar intermediate position is taken by existing data on Zn in Si.

For diffusion involving interstitial–substitutional exchange two models have been proposed. In the kick-out model the highly mobile, interstitially dissolved Zn_i atom gains an energetically more favourable place on the regular lattice (Zn_s) by pushing a Si atom into the interstice according to (Gösele *et al* 1980)

$$Zn_i \rightleftharpoons Zn_s + I \tag{1}$$

where I stands for self-interstitial. By contrast, in the dissociative model (Frank and Turnbull 1956) site interchange occurs under participation of lattice vacancies (V) as

$$Zn_s \rightleftharpoons Zn_i + V \tag{2}$$

Although at first glance the quasi-chemical reactions (1) and (2) look rather similar, the fact that the cooperating intrinsic defects (V or I) appear on different sides with respect to Zn_s induces a completely dissimilar diffusion behaviour. In the dissociative model the effective diffusivity of Zn_s in dislocation-free Si is described by

$$D_{\text{eff}}^{(V)} = \frac{C_V^{eq} D_V}{C_s^{eq}} \tag{3}$$

where C_V^{eq} and D_V denote the equilibrium concentration and diffusivity of vacancies, respectively, and C_s^{eq} means Zn_s solubility. On the other hand, the prediction of the kick-out theory reads

$$D_{\text{eff}}^{(I)} = \frac{C_I^{eq} D_I}{C_s^{eq}} \frac{1}{(C_s/C_s^{eq})^2} \tag{4}$$

showing a strong dependence on the local concentration C_s. The meaning of the self-interstitial-related quantities C_I^{eq} and D_I in this equation is self-explanatory. The expressions (3) and (4) hold provided that Zn_s dominates over Zn_i and moreover $C_s^{eq} \gg C_V^{eq}$ or C_I^{eq}, respectively.

The qualitative difference between (3) and (4) allows us to distinguish experimentally the kick-out mechanism from the dissociative mechanism or from other models predicting a constant diffusivity. Furthermore, these interstitial–substitutional diffusivities comprise the contributions of vacancies, $C_V^{eq} D_V$, or self-interstitials, $C_I^{eq} D_I$, to the uncorrelated self-diffusion coefficient of Si. This provides a second criterion to check the validity of (3) or (4).

A third test for the occurrence of interstitial–substitutional diffusion is given by the comparison between penetration profiles in dislocation-free and highly dislocated crystals. In the latter case both the dissociative model and the kick-out model predict a larger Zn_s diffusivity, i.e.,

$$D_{\text{eff}}^{(i)} = \frac{C_i^{eq} D_i}{C_s^{eq}} \tag{5}$$

which reflects that the diffusion process is governed by the solubility C_i^{eq} and diffusivity D_i of Zn_i. The reason for this is the fast dislocation-induced elimination or creation of

intrinsic point defects in the bulk, so that the incorporation rate of Zn_s is no longer delayed by the flux of V from the surface or of I towards the surface.

In this paper we will show that Zn diffuses in Si by the kick-out mechanism. It is found, however, that the appearance of this mechanism critically depends on the condition of the surface. Evidence for kick-out diffusion results from experiments on both dislocation-free and highly dislocated Si crystals, employing the spreading-resistance technique for penetration profile monitoring. With the aid of Hall effect measurements a new acceptor level which we ascribe to substitutional Zn has been detected in our diffused samples. Finally we will compare the present results with data from the literature.

2. Experimental

2.1. Silicon samples

In our experiments three types of samples were utilised which are designated below as 'thin', 'thick' and 'highly dislocated'. These samples are characterised as follows.

(i) Thin samples were dislocation free, either almost 1.0 mm or about 0.5 mm thick, and approximately 10×5 mm^2 in size. They are termed 'thin', since they were employed for measurements where the Zn profiles penetrating from both large surfaces overlapped in the middle. Thin samples were cut from $\langle 111 \rangle$-oriented float-zone wafers with a resistivity of 3 Ω m due to phosphorous doping. According to the manufacturer (Wacker Chemitronic) the wafers contained extremely low concentrations of carbon and oxygen, specified as $\leq 5 \times 10^{20}$ m^{-3} and $\leq 3 \times 10^{21}$ m^{-3}, respectively.

(ii) Thick samples were also dislocation free. They had cube-like shapes with edge lengths around 5 mm. The float-zone base material was boron doped to a resistivity of 17 Ω m. The average carbon content amounted to 5×10^{20} m^{-3} or less, whereas for oxygen a typical upper limit of 1×10^{22} m^{-3} applied. Thick samples were used when we wanted the diffusion-induced Zn distributions to drop to undetectably low values beyond a certain distance from the two $\langle 100 \rangle$ surfaces.

(iii) A highly dislocated sample possessed a dislocation density between 5×10^{11} m^{-2} and 2×10^{12} m^{-2}. This sample with a thickness of 1.5 mm was cut from a bar with dimensions $3.8 \times 3.8 \times 17$ mm^3 perpendicularly to the long axis pointing into the $\langle 213 \rangle$ direction. This bar which consisted of 30 Ω m boron-doped silicon had been plastically deformed by compression at 923 K. Details of the deformation procedure are given by Kisielowski-Kemmerich *et al* (1986).

2.2. Sample preparation and diffusion annealing

Initially Zn was diffused into well polished samples. However, after having analysed the resulting profiles we decided to use samples with damaged surfaces in later experiments. Damaging was done by scratching the front and back with a diamond tip. The purpose of this treatment was to produce a sufficient density of sinks for Si self-interstitials at the boundaries (see §3.1).

The samples were sealed in quartz ampoules with a volume of about 3×10^{-6} m^3 together with argon and 10–40 mg elemental Zn of 99.9999 % purity. This amount of Zn was taken in order to establish the equilibrium partial pressure of about 2×10^5 Pa at the diffusion temperature.

Annealing was performed in a resistance furnace and terminated by quenching the ampoules in water at room temperature. Subsequently the samples were cut perpendicularly to the faces in two about equal pieces. One of the so-obtained inner planes was prepared for the spreading-resistance measurement by the methods described elsewhere (Stolwijk *et al* 1985, 1986). Angle lapping as a means to profile stretching was not applied, since the Zn diffusion turned out to be rather fast.

In several cases the plane of the spreading-resistance measurement was etched to reveal the possible presence of diffusion-induced defects. For this purpose the procedure of Sirtl and Adler (1961) was followed.

2.3. Spreading-resistance technique

2.3.1. Profile measurement. Diffusion profiles were recorded by means of the spreading-resistance (R_s) technique. Details of this two-probe method are given by Mazur and Dickey (1966) and Stolwijk *et al* (1985, 1986).

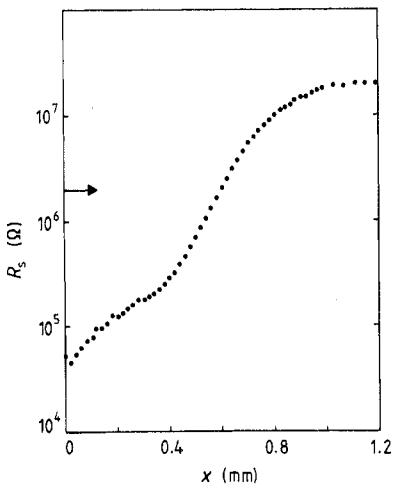

Figure 1. Spreading-resistance (R_s) profile measured on a 'thick' dislocation-free Si sample after 1.2 h of Zn diffusion at 1262 K. The arrow indicates the R_s value of the p-type base material corresponding to a resistivity of 17 Ω m.

Figure 1 shows a Zn-induced R_s profile measured on a thick Si sample. The arrow indicates the R_s value associated with the resistivity (17 Ω m) of the boron-doped starting material. Near the surface the spreading resistance is lowered due to in-diffusion of Zn. At greater depths the R_s data exceed the original value of 2×10^6 Ω, which implies that electrical compensation occurs. However, since Zn introduces one or maybe more acceptor levels into the already p-type material, some donor action must have been generated during diffusion annealing. Although the origin of this phenomenon is not quite clear, it has been taken into account by considering the new bulk R_s value of 2×10^7 Ω as representive of a changed effective background resistivity. By doing so the calculation of Zn concentrations in the 10^{19} m^{-3} regime is affected (§2.3.2). Fortunately, since the analysis of our profiles focuses on concentrations roughly between 10^{21} m^{-3} and 10^{20} m^{-3}, the influence of the above procedure is rather minor.

2.3.2. Conversion into concentration data. R_s data were converted into Zn_s concentrations (C_s) by solving the charge neutrality equation. At first we took into account two well established acceptor levels of Zn in Si, i.e. $E_v + 0.31$ eV and $E_c - 0.55$ eV (Fuller and Morin 1957, Carlson 1957, Chen and Milnes 1980; see also Bakhadyrkhanov *et al* 1970a, Herman and Sah 1972, 1973). Although the use of these levels already revealed most characteristic features of the Zn diffusion to be reported in §3, some of the results were not unambiguous. This prompted us to conduct Hall effect measurements yielding $E_v + 0.24$ eV as the main acceptor level in our Zn-diffused samples (see §2.4). This value which we attribute to Zn_s was then utilised in all further analyses. In addition, it was checked that the possible existence of a deep-lying second ionisation stage would have a negligible effect on the computed Zn_s concentrations.

In the calculation of C_s no allowance was made for vibrational entropy effects. Consequently only a degeneracy factor associated with the 0.24 eV level was taken into account. Considering that for boron the degeneracy factor equals 4 which results from a combination of valence band multiplicity and electron shell occupancy statistics, it was taken as unity for Zn. In the case of this divalent impurity, the two previously mentioned contributions to the degeneracy factor cancel each other.

In principle a correction was made for the influence of the ionised impurity concentration on the hole mobility. However, since our highest C_s values of about 2×10^{21} m^{-3} are still relatively low the effect of this correction turned out to be small.

Applying the above scheme of computation to the R_s data of figure 1 gives the lower concentration profile in figure 7.

2.4. Hall effect measurements

To determine the major Zn-related energy level(s) in our samples Hall effect analysis was applied. For this purpose a Si slice 500 μm thick consisting of 'type 1' base material as described in §2.1 was subjected to Zn diffusion treatment (1262 K, 0.83 h). The spreading-resistance profile recorded on a part of this sample showed a pronounced U-shape like that seen for similar measurements shown in figure 3. In order to obtain a fairly homogeneous Zn distribution 100 or 130 μm was taken off from the two plane surfaces by lapping. On the remaining inner slice with a thickness of 270 μm Ohmic contacts in van der Pauw geometry were fabricated. To this end evaporation of Al was followed by a 0.33 h anneal at 873 K. Then Hall effect analysis was performed with the equipment extensively described by Cohausz (1987).

The resulting hole concentration as a function of (reciprocal) temperature is displayed in figure 2. Here the full line indicates the range of data which has been taken for the determination of the predominant acceptor level. Correcting for the explicit temperature dependence of the valence band density of states as well as for its implicit temperature dependence through the effective mass of holes (Barber 1967) we found an electronic energy of 0.24 ± 0.02 eV above the valence band edge. This result is supported by the Hall measurement on a second Zn-diffused sample. Moreover, figure 2 suggests that the hole concentration saturates slightly above room temperature at about 8×10^{19} m^{-3}. This value agrees rather accurately with the average Zn concentration of the 270 μm wide central part of the sample as extracted from the spreading-resistance profile with the aid of this 0.24 eV level.

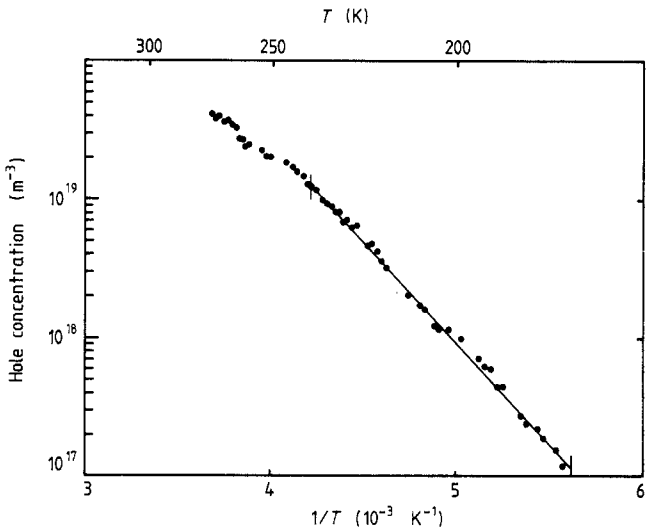

Figure 2. Hall effect measurement on the central part of a Zn-diffused silicon slice. The full line marks the range of data from which the acceptor energy of 0. 24 eV was calculated.

3. Results and analysis

3.1. Thin samples

Figure 3 reveals Zn_s profiles which were measured after annealing at 1262 K for different periods of time. All profiles extend throughout the entire cross section of the dislocation-free Si plates with thicknesses d around 900 μm. Whereas the lowest curve arises from a 0.55 h treatment, the almost flat, upper profile was obtained after almost six days of annealing. In the latter case the sample was deliberately chosen half as thick (470 μm) as the other ones in order to get a reliable estimate for the Zn_s solubility at 1262 K after a reasonable time interval.

For a trained eye the concentration–depth curves in figure 3 look rather peculiar. Common erfc-type profiles exhibit a concave shape near the boundaries when the logarithm of concentration is plotted against penetration depth x. In other words, given the presence of Zn in the wafer centre, a constant diffusion coefficient would have produced points of inflection in both halves of the profile. On the other hand, the observed convex appearance is reminiscent of similar distributions found for Au in Si. Since the present data also show that the diffusion rates of Zn and Au are comparably fast, an interpretation in terms of the kick-out mechanism presents itself naturally.

Another finding which guided us to the kick-out hypothesis is the following. In several experiments we saw penetration profiles which resembled the complementary error function. In these cases the diffusion fronts entering the sample from both sides had not reached the centre, so that no overlap occurred. We found out that such erfc-like profiles could be avoided by damaging the surfaces prior to diffusion (see §2.2). After having introduced this treatment kick-out-like distributions were always observed (see figure 3).

The idea behind surface damaging was that for some unknown reason self-

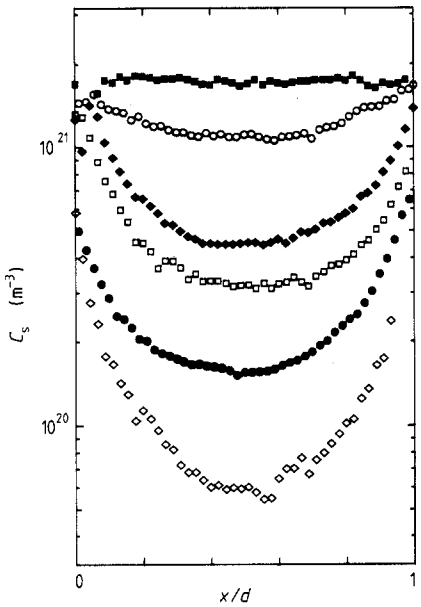

Figure 3. Six of nine available Zn_s profiles in 'thin' Si wafers showing the rise of the bulk concentration with increasing duration of annealing at 1262 K (0.55 h, 2.00 h, 7.88 h, 16.9 h, 126.4 h, 126.8 h). Wafer thicknesses lie between 880 and 940 μm, except for the upper most profile which belongs to a 470 μm thick sample.

interstitials originating from the Zn_i-to-Zn_s transformation are not able to annihilate at well polished surfaces in contact with the Zn vapour. Since sinks for self-interstitials are also absent in the dislocation-free interior, an I supersaturation will persist and hinder further incorporation of Zn. (In support of this we note that our samples remained free of dislocations during diffusion as was checked by etching techniques.) Hence the kick-out process will stop shortly after the beginning of the diffusion anneal. However, by scratching the surfaces, kick-out diffusion will go on since the generated self-interstitials can leave the crystal through 'permeable' boundaries.

To verify the supposition that the profiles in figure 3 represent diffusion via the kick-out mechanism they are subjected to a closer inspection in the following subsections.

3.1.1. Depth dependence. First we compare the shape of the profiles with the prediction of the kick-out model (Gösele *et al* 1980)

$$\operatorname{erf}\left(\ln \frac{C_s}{C_s^m}\right)^{1/2} = \left|\frac{d/2 - x}{d/2}\right| \tag{6}$$

where $C_s^m = C_s(x = d/2)$ denotes the Zn_s concentration in the middle of the wafer with thickness d. For the second lowest profile of figure 3 such a comparison is shown in figure 4. It is seen that the experimental data are well described by (6) which in this special plot appears as the straight line with slope 1.

In order to judge the degree of correspondence between measured profile and kick-out theory the following remarks may be helpful.

(i) The observed agreement in figure 4 is *not* the result of some fitting procedure, since there are no adjustable parameters in (6).

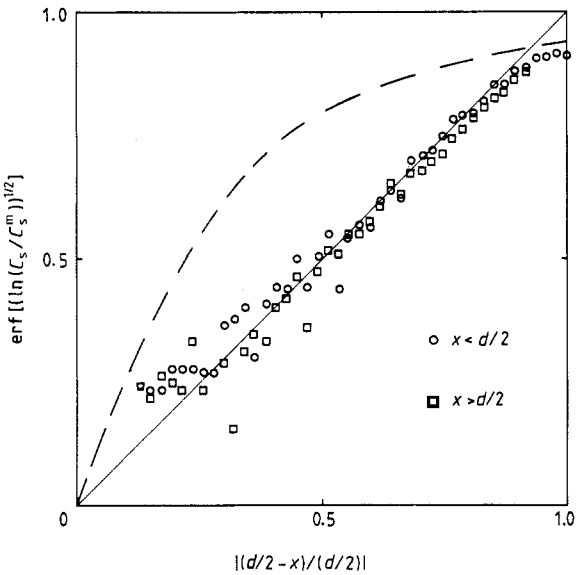

Figure 4. The shape of an experimental Zn_s profile in a 'thin' Si wafer compared with the prediction from kick-out theory (full line). The broken curve represents an erfc-type profile.

(ii) The scatter of the data on the lower left-hand side is due to the fact that small fluctuations in $C_s \simeq C_s^m$ are magnified by the mathematical operation given in the left-hand side of (6).

(iii) The systematic departure of the data from the straight line in the upper right part of figure 4 reflects the finite boundary concentration C_s^{eq}, whereas in the derivation of (6) the approximation $C_s(0) = C_s(d) = \infty$ has been made (Gösele *et al* 1980).

(iv) The broken curve represents diffusion models which predict a concentration-independent diffusivity. Here the relevant solution (Crank 1975) of Fick's second law was 'fitted' to C_s^m and C_s^{eq}.

3.1.2. Time dependence. As a second check for the validity of the kick-out model we analyse the rate at which the concentration in the wafer centre increases. Figure 5 reveals that the data obey a $\sqrt{t}$ law which in this double-logarithmic diagram is given by the straight line with slope $\frac{1}{2}$. This agrees with the kick-out expression

$$\frac{C_s^m}{C_s^{eq}} = \left(4\pi D_I^* \frac{t}{d^2}\right)^{1/2} \tag{7}$$

where

$$D_I^* = \frac{C_I^{eq} D_I}{C_s^{eq}} \tag{8}$$

may be considered as the effective Zn_s diffusivity for $C_s = C_s^{eq}$. This solubility was determined from the profile in figure 3 associated with the longest annealing time as 1.75×10^{21} m^{-3}, in fair agreement with literature data (Blouke *et al* 1970). The best fit of (7) to the data (full line in figure 5) yields $D_I^* = 5.9 \times 10^{-14}$ m^2 s^{-1}. In contrast, the broken line in figure 5 forms a clear demonstration that an erfc-like increase of C_s^m based on a constant diffusivity is not able to reproduce the experimental behaviour.

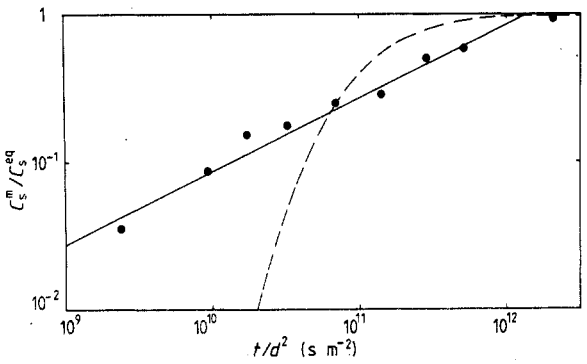

Figure 5. Time dependence of the Zn_s concentration C_s^m in the middle of 'thin' Si wafers revealing kick-out diffusion behaviour (full line). The broken curve results from the overlapping of two erfc profiles which enter the wafer from both sides.

3.1.3. Comparison with Si self-diffusion coefficients. A third test for the occurrence of kick-out diffusion results from a calculation of the self-interstitial contribution $C_I^{eq}D_I$ to the (uncorrelated) Si self-diffusion coefficient. Based on (4) and (8) this quantity can be determined from the solubility and diffusivity of Zn according to

$$C_I^{eq}D_I = C_s^{eq}D_I^*. \tag{9}$$

Inserting into the right-hand side of (9) the values given in the previous subsection we obtain $C_I^{eq}D_I = 2.1 \times 10^{-21}$ m^2 s^{-1}. In figure 6 the present result (cross) is plotted together with self-diffusion coefficients D^T from the literature, which originate from direct measurements with the aid of Si tracers (open symbols). For this purpose our value was multiplied by $\frac{1}{2}$, which is an arbitrary estimate for the correlation factor connected with tracer self-diffusion via the interstitial mechanism. Also $\frac{1}{2}C_I^{eq}D_I$ data, which have previously been extracted from the kick-out diffusion of Au and Pt in Si (Frank and Stolwijk 1987), are displayed in figure 6 (full symbols). The observed accordance between the result of this work and the other self-diffusion data provides additional evidence that the kick-out mechanism operates for Zn in Si.

3.2. Thick samples

3.2.1. Highly dislocated case. The upper profile in figure 7 was recorded after in-diffusion of Zn during 1.2 h into a Si sample with a dislocation density of about 10^{12} m^{-2}. This sample with a thickness of 1.3 mm may be regarded as 'thick', because hardly any interference of the displayed profile with that of the other sample half was seen. Figure 7 shows that the experimental data are fairly well matched by the complementary error function (full curve). This is precisely what the kick-out theory predicts on the basis of the concentration-independent $D_{eff}^{(i)}$ given in (5). This Zn_i-controlled diffusivity holds in the case of a high density of sinks for self-interstitials in the bulk, so that C_I is vitually equal to C_I^{eq}. Using (5) the influx of Zn_i atoms, $C_i^{eq}D_i$, is calculated as

$$C_i^{eq}D_i = C_s^{eq}D_{eff}^{(i)} \tag{10}$$

where both $C_s^{eq} = 2.07 \times 10^{21}$ m^{-3} as represented by the boundary concentration and $D_{eff}^{(i)} = 4.6 \times 10^{-12}$ m^2 s^{-1} result from the best erfc fit (full curve) to the data. This

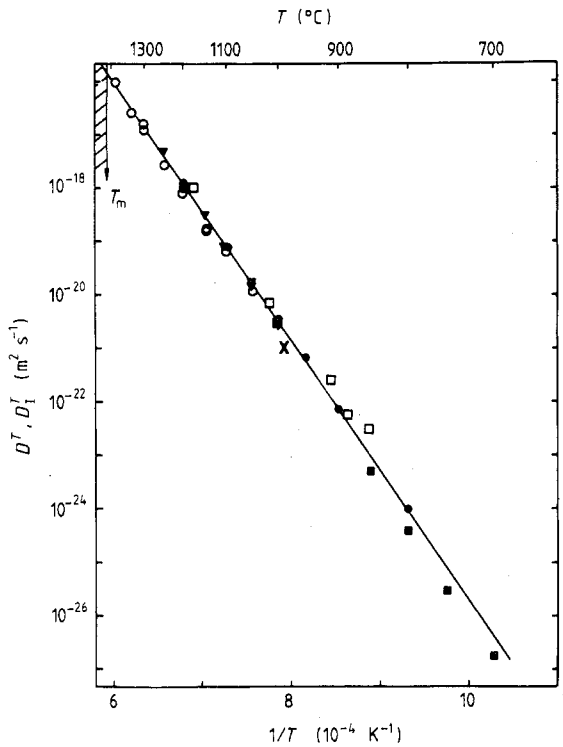

Figure 6. Self-diffusion coefficients of Si. D^T data result from direct measurements using Si tracers: open circles, Mayer *et al* (1976); open squares: Kalinowski and Seguin (1979). Values of $D_I^T = \frac{1}{2}C_I^{eq}D_I$ have been calculated from the solubility and diffusivity of impurities which migrate by the kick-out mechanism: full circles, Au (Stolwijk *et al* 1984, 1986); full inverted triangles, Pt (Hauber 1986); full squares, Pt (Mantovani *et al* 1986); cross, Zn (this work).

yields $C_i^{eq}D_i(1262\ \text{K}) = 1.9 \times 10^{-19}\ \text{m}^2\ \text{s}^{-1}$ which is about a factor of 100 larger than $C_I^{eq}D_I$ at the same temperature (see §3.1.3). This demonstrates the self-consistency in our findings, since

$$C_i^{eq}D_i \gg C_I^{eq}D_I \tag{11}$$

is a key assumption made in the derivation of the self-interstitial-limited diffusivity (4) governing Zn transport in dislocation-free Si.

3.2.2. Dislocation-free case. The lower profile in figure 7 originates from a 5 mm thick, dislocation-free Si sample which has been subjected to the same diffusion treatment (1262 K, 1.2 h) as the highly dislocated crystal above. Near the boundary the profile exhibits the convex shape which is characteristic for kick-out diffusion in a matrix without inner sinks for self-interstitials. This portion is well reproduced by the theoretical profile (broken curve) for a C^{-2}-dependent diffusivity in a semi-infinite crystal (Seeger 1980). When the C_s^{eq} value from the highly dislocated case is adopted, least-squares fitting yields $D_I^* = 1.5 \times 10^{-13}\ \text{m}^2\ \text{s}^{-1}$. Using (5) one finds $C_I^{eq}D_I = 6.2 \times 10^{-21}\ \text{m}^2\ \text{s}^{-1}$ which is somewhat larger than the result from the thin-sample experiments and therefore agrees even better with the literature data. Nevertheless we are more confident

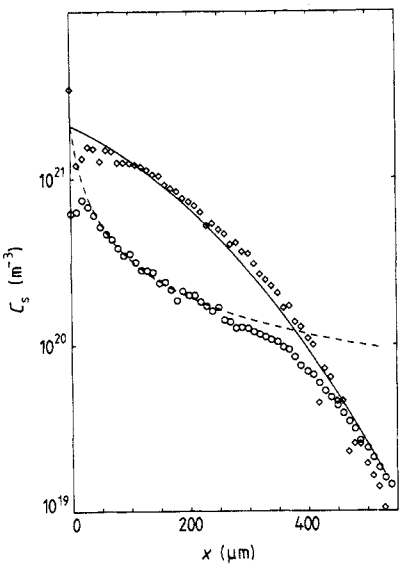

Figure 7. Zn_s profiles after 1.2 h anneals at 1262 K in dislocation-free (open circles) and highly dislocated (open diamonds) Si. The full curve is an erfc-fit to the upper data yielding $D_{eff}^{(I)}$. The broken curve represents a $D_{eff}^{(I)}$-induced distribution adjusted to the lower data.

in our earlier value displayed in figure 6 (cross) since it is based on a series of nine penetration profiles (figure 3) instead of one. In addition, the present analysis may suffer from uncertainties due a down turn of the experimental profile which is seen in figure 6 to set in at a penetration depth of about 350 μm.

Now we will discuss why the Zn_s profile in a thick dislocation-free sample changes its shape at greater depths thereby tending to approximate to the erfc-profile of a highly dislocated crystal.

Near the surface the incorporation of Zn_s is governed by the outflux of self-interstitials. This is expressed by (4) which has been derived under the assumption $C_i = C_i^{eq}$ (Gösele *et al* 1980). However, because of its dependence on C_s^{-2} the self-interstitial-limited diffusivity becomes faster the more C_s decreases. As a consequence the supply of Zn_i from the surface cannot keep up below some critical concentration $C_s^{(c)}$. Then, for $C_s < C_s^{(c)}$ the penetration rate is controlled by $D_{eff}^{(i)}$ given in (4). The concentration where the change-over from self-interstitial- to Zn_i-controlled diffusion takes place is approximately given by the point of intersection between the broken curve and the full curve in figure 7. Indeed, at about this C_s level the lower measured profile changes the sign of its curvature. This shows that the departure from the broken curve in figure 7 also fits in with the theory of the kick-out mechanism.

4. Discussion

4.1. Possibility of diffusion-induced generation of defects

In the foregoing it was shown that our measured diffusion profiles of Zn in Si agree with the predictions of the kick-out model. In the case of dislocation-free samples this agreement implies that Zn diffusion has taken place under virtually perfect conditions,

since kick-out diffusion is sensitive for the occurrence of sinks for self-interstitials in the bulk of the crystal. This conclusion is supported by the fact that no etch pitches were observed on the plane of the spreading-resistance measurement after diffusion.

The situation depicted above is reminiscent of Si:Au. Penetration of this noble metal into undeformed floating-zone material is mostly well described by theoretical kick-out profiles for a crystal without inner sinks. Departures from this ideal behaviour could always be related to the appearance of diffusion-induced defects, i.e. stacking faults (Hauber *et al* 1986). Also in as-grown Czochralski wafers anomalies of the Au diffusion are only found in connection with the creation of crystal defects during diffusion (Stolwijk *et al* 1987).

In contrast to Si:Au and Si:Zn, the diffusion of Zn in GaAs involves the generation of a high density of defects such as dislocation loops and Ga-rich precipitates (Stolwijk *et al* 1988, Luysberg *et al* 1989). This pronounced effect may be related to the high solubility of Zn in GaAs which is at least a factor of 1000 higher than in Si. In addition, GaAs is less perfect than Si so there will be enough nuclei in the crystal for defect growth. These circumstances may favour local agglomeration of the substituted Ga atoms over long-distance migration to the surface. Inversely, the profile shape and the absence of etch pitches in the present study show that, in dislocation-free Si, self-interstitials produced by the incorporation of Zn annihilate at the surface rather than being trapped in the interior of the crystal.

4.2. Kick-out reaction rates

The derivation of the effective diffusion coefficients (3), (4) and (5) relies on the quasi-chemical reactions (1) and (2). Strictly speaking, the mass action law can only be applied to systems which are in equilibrium. Diffusion is inherently a non-equilibrium process. Therefore, the effective diffusivities given in the introduction only hold if the reaction rates associated with the Zn_i–Zn_s interchange are much faster than any diffusion process.

Our measured penetration profiles are well described by the solution of the diffusion equation (Fick's second law) based on the kick-out diffusivities (4) or (5). This shows that the above condition is fulfilled for Zn diffusion at 1262 K into both dislocation-free and highly dislocated Si, at least to a good approximation.

4.3. Comparison with literature data

Several studies of the Zn diffusion in Si have been published. We will summarise the main results of these older experiments and discuss them in the light of the present findings.

Fuller and Morin (1957) measured the conductivity of their samples after in- or out-diffusion of Zn in the temperature range 1273–1573 K. The diffusivities so obtained varied between 10^{-10} and 10^{-11} m^2 s^{-1}, but the large scatter prevented them establishing a definite trend with temperature. The authors attribute this to oxide films on the surface acting as diffusion barriers. The analysis of the measurements is based on the error function. Unfortunately, the validity of this assumption cannot be checked since no penetration profiles are produced by their experimental technique. Presumably the data of Fuller and Morin are representative of $D_{\mathrm{eff}}^{(i)}$ which controls the deepest Zn penetration (see the great-depth part of the lower profile in figure 7). Note that their smallest value of 10^{-11} m^2 s^{-1} is not much different from our $D_{\mathrm{eff}}^{(i)}$ result (4.6×10^{-12} m^2 s^{-1} at 1262 K). On the other hand, a similar analysis to that of Fuller

and Morin applied to the $D_{eff}^{(I)}$-controlled profiles of figure 3 would also yield diffusion coefficients of comparable magnitude. Although this approach is not justified in view of the concentration-dependent diffusivity observed in our work, it provides a possible 'explanation' of the older data.

Malkovich and Alimbarashvili (1963) performed electro-transport experiments between 1253 and 1543 K. They report Zn diffusivities running from 3×10^{-11} m^2 s^{-1} at the lowest temperature to 3×10^{-10} m^2 s^{-1} at the highest, however, without presenting diffusion profiles. Since these features are similar to those given by Fuller and Morin, much of what has been said above also holds here. From the influence of the electric field an effective Zn charge of almost 2.0 was extracted which indicates that the moving species is Zn_i. This provides additional evidence that $D_{eff}^{(i)}$ data were determined. Also the reported dislocation density in excess of 10^8 m^{-2} would favour the Zn_i-controlled diffusion mode, since a sufficiently dense network of dislocations shortens the trajectories for self-interstitial elimination (Stolwijk *et al* 1986, 1987).

Also Bakhadyrkhanov *et al* (1970b) find Zn diffusivities in the $10^{-11} - 10^{-10}$ m^2 s^{-1} regime, i.e. for temperatures between 1373 and 1573 K. Their observation that the measured radiotracer profiles cannot be described by the erfc function is interesting. Their D values were estimated from the increase of the almost uniform bulk concentration as a function of annealing time. This may point to Zn distributions like those in figure 3 which vary slowly in the interior of the wafers when plotted on a linear scale. The presence of dislocations (10^7–10^8 m^{-2}) in the samples of Bakhadyrkhanov *et al* could have made their profiles even flatter (Stolwijk *et al* 1987).

Koifman and Niyazova (1972) investigated both the diffusion of Au and Zn under neutron and γ irradiation at 400 K in a nuclear reactor. An extremely high Zn diffusivity was found at this relatively low temperature, which they interpret as being due to γ-radiation enhancement. Although these findings are not well understood, the observed similarity between the behaviour of Zn and Au is in line with our results.

In the work of Zalar (1970) the influence of quite a few variables on the Zn diffusion in Si was examined: duration of annealing, type of silicon, diffusion temperature (1173–1373 K), temperature of the Zn source (873–1173 K) and chemical treatment of the sample surface. However, no reference is made to dislocation densities. Applying the spreading-resistance technique Zalar obtains erfc-like profiles at 1273 K yielding a diffusivity of 4.4×10^{-12} m^2 s^{-1}. This value is practically equal to our result for $D_{eff}^{(i)}$ at 1262 K.

The reason why in the presumably (almost) dislocation-free samples of Zalar the convex-profile part near the surface has not been observed (or possibly overlooked) may be due to the low temperature (973 K) at which the Zn source was kept. Namely, by separately controlling the sample and source temperature it was possible to establish much smaller partial Zn pressures than in our experiment. This does not affect $D_{eff}^{(i)}$ since this diffusion coefficient contains a Zn solubility in the numerator (C_i^{eq}) as well as in the denominator (C_s^{eq}). However, $D_{eff}^{(I)}$ increases when, by reducing the Zn pressure, C_s^{eq} is reduced. One may also say that the difference between $C_I^{eq}D_I$ and $C_i^{eq}D_i$ becomes smaller because C_i^{eq} is lowered. This will restrict the self-interstitial-limited, non-erfc portion of the Zn_s profile in dislocation-free Si to a narrower region beneath the surface or even lead to its complete disappearance. (In figure 7 the effect under consideration would show up as a shifting of the point of intersection between the full and broken curves to higher C_s values and concomitantly to shallower penetrations.)

Another explanation for the erfc-like profiles found by Zalar arises if one assumes that the surface of his samples were not effective as sinks for self-interstitials, as

discussed with respect to our undamaged crystals in §2.2. Supposing further that Zn diffuses simultaneously by the kick-out mechanism and the dissociative mechanism, as has been shown for Au (Morehead *et al* 1983) and, moreover, that the boundaries always provide sufficient sources for vacancies, then the Zn_s incorporation is governed by $D_{\text{eff}}^{(V)}$ as given in (3). Analogously, this vacancy-controlled diffusion constant could be responsible for the erfc-shaped profiles in our preliminary experiments.

The above interpretation receives support from Zalar's observation that surface cleaning and etching affect the diffusion behaviour. The author speaks of 'accelerated' and 'exceptionally high' diffusion after using an extended chemical treatment prior to annealing. Remarkably, the corresponding profiles given by Zalar in his figures 8 and 9 reveal some resemblance with the $D_{\text{eff}}^{(I)}$-determined distributions in our figure 3. Apparently, the extended treatment of Zalar and the scratching in the present work have the same effect, i.e. the opening of the surface for self-interstitial annihilation. We note further that $C_I^{eq} D_I$ and $C_V^{eq} D_V$ are of comparable magnitude around 1273 K (Morehead *et al* 1983). Consequently, an unhindered contribution of self-interstitials to Zn_s migration in addition to a vacancy component as enabled by surface conditioning will automatically lead to the predominance of the kick-out mechanism owing to the factor $(C_s/C_s^{eq})^{-2} \gg 1$ in the expression for $D_{\text{eff}}^{(I)}$.

Summarising the literature on Si:Zn, it is concluded that most of the earlier diffusion data are compatible with the present findings. Nevertheless, the role of the surface and the participation of vacancies in Zn transport need more clarification.

5. Conclusions

An acceptor level lying 0.24 eV above the valence band edge has been detected in Zn-diffused Si. This level is attributed to Zn atoms in a substitutional configuration.

Surface conditions play an important role for the diffusion behaviour of Zn into Si.

In Si crystals with damaged surfaces Zn transport proceeds by the kick-out mechanism. This conclusion is based on the following observations.

(i) The (non-erfc) shape of the Zn distribution in dislocation-free wafers is consistent with a diffusivity proportional to C^{-2}.

(ii) The increase of the Zn concentration in the centre of thin dislocation-free samples obeys a $\sqrt{t}$ law.

(iii) Si self-diffusion coefficients calculated within the framework of the kick-out theory from the diffusivity and solubility of Zn agree with literature data.

(iv) Diffusion of Zn in highly dislocated Si is much faster than in dislocation-free samples and characterised by ordinary erfc-profiles.

Acknowledgments

We thank Dipl. Phys. M Brohl and Professor H Alexander (University of Köln) for the donation of a plastically deformed Si crystal. We are indebted to Professor H Mehrer for his stimulating support and for reading the manuscript. The advice of Dipl. Phys. D Grünebaum concerning the experiments was very much appreciated.

References

Bakhadyrkhanov M K, Boltaks B I, Dzhafarov T D and Kulikov G S 1970a *Sov. Phys.–Solid State* **11** 3076

Bakhadyrkhanov M K, Boltaks B I, Kulikov G S and Pedyash E M 1970b *Sov. Phys.–Semicond.* **4** 739
Barber H D 1967 *Solid-State Electron.* **10** 1039
Blouke M M, Holonyak N Jr, Streetman B G and Zwicker H R 1970 *J. Phys. Chem. Solids* **31** 173
Carlson R O 1957 *Phys. Rev.* **108** 1390
Chen J W and Milnes A G 1980 *Ann. Rev. Mater. Sci.* **10** 157
Cohausz L 1987 *Dr. rer. nat. thesis* University of Kassel
Crank J 1975 *Mathematics of Diffusion* (Oxford: Clarendon) p 48
Frank F C and Turnbull D 1956 *Phys. Rev.* **104** 617
Frank W and Stolwijk N A 1987 *Mater. Sci. Forum* **15–18** 369 (transl. Tech Publications, Switzerland)
Fuller C S and Morin F J 1957 *Phys. Rev.* **105** 379
Gösele U, Frank W and Seeger A 1980 *Appl. Phys.* **23** 361
Hauber J, Frank W and Stolwijk N A 1989 *Mater. Sci. Forum* **38–41** 707 (transl. Tech Publications, Switzerland)
Hauber J, Stolwijk N A, Tapfer L, Mehrer H and Frank W 1986 *J. Phys. C: Solid State Phys.* **19** 5817
Herman J M and Sah C T 1972 *Phys. Status Solidi* a **14** 405
—— 1973 *J. Appl. Phys.* **44** 1259
Kalinowski L and Seguin R 1979 *Appl. Phys. Lett.* **35** 211
—— 1980 *Appl. Phys. Lett.* **36** 171
Kisielowski-Kemmerich C, Czaschke J and Alexander H 1986 *Mater. Sci. Forum* **10–12** 745 (transl. Tech Publications, Switzerland)
Koifman A I and Niyazova D R 1972 *Phys. Status Solidi* a **10** 59
Luysberg M, Jäger W, Urban K, Perret M, Stolwijk N A and Mehrer H 1989 *Proc. 6th Conference on Microscopy of Semiconducting Materials (Oxford), Inst. Phys. Conf. Series* in press
Malkovich R Sh and Alimbarashvili N A 1963 *Sov. Phys.–Solid State* **4** 1725
Mantovani S, Nava F, Nobili C and Ottaviani G 1986 *Phys. Rev.* **33** 5536
Mayer H J, Mehrer H and Maier K 1977 *Radiation Effects in Semiconductors 1976 (Int. Phys. Conf. Ser. 31)* p 186
Mazur R G and Dickey D H 1966 *J. Electrochem. Soc.* **113** 255
Morehead F, Stolwijk N A, Meyberg W and Gösele U 1983 *Appl. Phys. Lett.* **42** 690
Seeger A 1980 *Phys. Status Solidi* a **61** 521
Sirtl E and Adler A 1961 *Z. Metallk.* **52** 529
Stolwijk N A, Hölzl J, Frank W, Hauber J and Mehrer H 1987 *Phys. Status Solidi* a **104** 225
Stolwijk N A, Hölzl J, Frank W, Weber E R and Mehrer H 1986 *Appl. Phys.* **39** 37
Stolwijk N A, Perret M and Mehrer H 1988 *Defect and Diffusion Forum* **59** 79 (transl. Tech Publications, Switzerland)
Stolwijk N A, Schuster B and Hölzl J 1984 *Appl. Phys.* A **33** 133
Stolwijk N A, Schuster B, Hölzl J, Mehrer H and Frank W 1983 *Physica* B **116** 335
Zalar S M 1970 *J. Appl. Phys.* **41** 3458